

**H<sub>2</sub>O and other hydrogen-oxygen compounds at giant-planet core pressures**Shuai Zhang,<sup>1,\*</sup> Hugh F. Wilson,<sup>1</sup> Kevin P. Driver,<sup>1</sup> and Burkhard Militzer<sup>1,2,†</sup><sup>1</sup>*Department of Earth and Planetary Science, University of California, Berkeley, California 94720, USA*<sup>2</sup>*Department of Astronomy, University of California, Berkeley, California 94720, USA*

(Received 15 September 2012; revised manuscript received 17 January 2013; published 31 January 2013)

Water and hydrogen at high pressure make up a substantial fraction of the interiors of giant planets. Using *ab initio* random structure searching methods we investigate the ground-state crystal structures of water, hydrogen, and hydrogen-oxygen compounds. **We find that, at pressures beyond 14 Mbar, a novel phase with H<sub>2</sub>O stoichiometry is stable relative to separate water ice and hydrogen phases.** We also predict two new ground-state structures,  $P2_1/m$  and  $I4/mmm$ , for post- $C2/m$  water ice.

DOI: [10.1103/PhysRevB.87.024112](https://doi.org/10.1103/PhysRevB.87.024112)

PACS number(s): 64.70.K-, 61.50.Ah, 62.50.-p, 96.15.Nd

As one of the most abundant substances in the solar system, water ice at high pressure<sup>1,2</sup> is of fundamental importance in planetary science.<sup>3</sup> Over the last two years, a significant effort has been devoted to finding the ground-state structures of ice at the megabar pressures corresponding to the cores of gas giant planets (15–20 Mbar for Saturn and 40–60 Mbar for Jupiter). Militzer and Wilson<sup>4</sup> demonstrated that the  $Pbcm$  phase<sup>2</sup> becomes unstable above 7.6 Mbar and predicted a new structure of  $Pbca$  symmetry. Wang *et al.*<sup>5</sup> showed that, at 8.1 Mbar, water ice assumes another structure of  $I42d$  symmetry instead of transforming into a  $Cmcm$  structure as proposed in Ref. 4. References 6–8 instead proposed a structure with  $Pmc2_1$  symmetry to appear in the same pressure regime, but it has a higher enthalpy than the  $I42d$  structure. Around 12 Mbar, a transition to a structure with  $P2_1$  symmetry was consistently predicted in Refs. 5–8. At even higher pressures, studies predict a  $P2_1/c$  structure to emerge at 20 Mbar,<sup>7</sup> and a metallic  $C2/m$  structure at 60 Mbar.<sup>6,8</sup>

In nature, however, high-pressure water phases are rarely found in isolation, and, in gas giants, an icy core may be surrounded by a vast reservoir of hydrogen-rich fluid or exist in a mixture with the other planetary ices, such as ammonia and methane. Recent work has emphasized the fact that counterintuitive stoichiometries can occur in post-perovskite materials at extreme pressures.<sup>9</sup> This raises the question of whether H<sub>2</sub>O is indeed the ground-state stoichiometry for water at high pressure in hydrogen-rich environments, or whether pressure effects are likely to result in the formation of novel ice-like phases with non-H<sub>2</sub>O stoichiometry.

In this study, we apply *ab initio* random structure searching (AIRSS) methods<sup>10</sup> to determine the ground-state structure of hydrogen-oxygen compounds at extreme pressure, to explore whether the H<sub>2</sub>O stoichiometry of water is maintained at high pressure. The AIRSS method relies on the generation of a large number of random geometries whose structures are then optimized using density functional theory. In the AIRSS process, randomly generated unit cells are filled with randomly positioned atoms, and the structures are geometrically relaxed to the targeted pressure. Structures with competitive enthalpy are picked out and reevaluated with more accurate thermodynamic calculations, from which the most stable structure is determined. Although the AIRSS method is not guaranteed to find the most stable phase, it has achieved remarkable success in discovering structures across a wide range of materials.<sup>11–13</sup>

In our calculations, structural optimization is performed using the Vienna *ab initio* simulation package (VASP).<sup>14</sup> Projector augmented wave (PAW) pseudopotentials<sup>15</sup> and the Perdew-Burke-Ernzerhof<sup>16</sup> exchange-correlation functional are used. The pseudopotential cutoff radii are 0.8 and 1.1 Bohr for H and O. For efficiency of the AIRSS method, a cutoff energy of 900 eV is chosen for initial relaxation, which is then increased to 1700 eV for precise calculations on favorable structures. Likewise, a relatively sparse Monkhorst-Pack grid<sup>17,18</sup> ( $6 \times 6 \times 6$ ) is used initially, which is later replaced by a  $20 \times 20 \times 20$  grid. Tests at the largest energy cutoff and grid size show that the total system energies are converged to the order of 1 meV/molecule, while the energy difference is converged to 0.1 meV/molecule.

**As an initial step, we recomputed enthalpies of recently reported<sup>4–7</sup> H<sub>2</sub>O structures as a function of pressure, assembling all proposed structures for comparison. Figure 1 shows the transition sequence up to the highest reported pressure (70 Mbar) as follows:  $X \rightarrow Pbcm \rightarrow Pbca \rightarrow I42d \rightarrow P2_1 \rightarrow P2_1/c \rightarrow C2/m$ ,** consistent with previous reports. Note that the  $Pmc2_1$  structure predicted in Refs. 6–8 is less stable than the  $I42d$  structure reported by Wang *et al.*<sup>5</sup> at all pressures; as the  $I42d$  structure has eight formula units (f.u.) per unit cell, it was less likely to be generated by random search algorithms.

With a quickly increasing number of known massive exoplanets, it is worthwhile to explore stable H<sub>2</sub>O structures at even higher pressure. We use the AIRSS method to generate between 1000 and 3500 H<sub>2</sub>O unit cells with 1–4 f.u. at pressures of 100, 150, 300, 400, and 500 Mbar. Additionally, we generate between 750 and 1150 structures with 5–8 f.u. at pressures of 100 and 200 Mbar. Note that the number of structures generated here is comparable to recent reports on the AIRSS method.<sup>19,20</sup>

Figure 1 shows two new, stable phases with  $P2_1/m$  and  $I4/mmm$  symmetry that appear at high pressure. More stable than  $C2/m$  above 135 Mbar, the  $P2_1/m$  phase is also a monoclinic, layered structure that resembles the  $C2/m$  phase except that O–H–O bonds are divided into two classes: one is shortened and straight, while the other is squeezed and distorted in different directions. At 330 Mbar,  $P2_1/m$  is replaced by a tetragonal  $I4/mmm$  phase, which has the same structure as the  $L'2$  phase of ThH<sub>2</sub>.<sup>21</sup>  $I4/mmm$  remains the most stable structure up to 500 Mbar. Similar to the  $C2/m$  structure, an analysis of the electronic band

TABLE I. Structural parameters of selected H, H<sub>2</sub>O, H<sub>3</sub>O, and H<sub>4</sub>O phases.

Structure name No. of atoms	Pressure (Mbar)	Lattice parameters $a, b, c$ (Å) $\alpha, \beta, \gamma$ (deg.)	Atomic positions (fractional)			
H: <i>Cmcm</i> 4	60	0.935, 1.459, 1.317 90, 90, 90	H:	1/2	0.1642	1/4
H: hcp ( <i>P6<sub>3</sub>/mmc</i> ) 2	120	0.719, 0.719, 1.136 90, 90, 120	H:	2/3	1/3	3/4
H <sub>2</sub> O: <i>P2<sub>1</sub>/m</i> 12	250	1.866, 1.398, 1.941 90, 103.884, 90	H1:	0.6459	3/4	0.9253
			H2:	0.4006	3/4	0.6320
			H3:	0.0188	1/4	0.2515
			H4:	0.9084	1/4	0.6569
			O1:	0.7537	1/4	0.9484
			O2:	0.2662	1/4	0.5733
H <sub>2</sub> O: <i>I4/mmm</i> 6	400	1.378, 1.378, 1.032 90, 90, 90	H:	1/2	0	1/4
			O:	0	0	1/2
H <sub>3</sub> O: <i>Cmmm</i> 24	80	2.295, 1.633, 3.797 90, 90, 90	H1:	0.2849	0	0.3184
			H2:	0	0	1/2
			H3:	1/2	0	0.9136
			H4:	0.2351	0	0
			O1:	0	0	0.1928
			O2:	1/2	0	1/2
H <sub>3</sub> O: <i>C2/m</i> 32	100	5.275, 1.553, 3.595 90, 144.354, 90	H1:	0.0416	1/2	0.1392
			H2:	0.3298	1/2	0.4729
			H3:	0.8928	1/2	0.3238
			H4:	0.9839	1/2	0.7340
			H5:	0.4374	1/2	0.0613
			H6:	0.1548	1/2	0.0616
			O1:	0.7166	1/2	0.3090
			O2:	0.6040	1/2	0.7693
H <sub>3</sub> O: bcc ( <i>Im<math>\bar{3}m</math></i> ) 8	140	1.542, 1.542, 1.542 90, 90, 90	H:	0	0	1/2
			O:	0	0	0
H <sub>4</sub> O: <i>Pnma</i> 20	100	2.804, 1.563, 2.213 90, 90, 90	H1:	0.8538	3/4	0.1977
			H2:	0.6232	3/4	0.9150
			H3:	0.0612	3/4	0.2068
			H4:	0.5201	1/4	0.4692
			O:	0.8202	3/4	0.6306

structure shows that the *P2<sub>1</sub>/m* and *I4/mmm* phases are metallic. Structural parameters of these two phases are listed in Table I.

In addition to our initial studies on water ice, we used the AIRSS method to investigate hydrogen (for results see Fig. 2). Below 50 Mbar we find the same progression of ground-state structures, *Cmca*  $\rightarrow$  *C2/c*  $\rightarrow$  *I4<sub>1</sub>/amd* (or *Fddd*)  $\rightarrow$  *Cmcm*, as has been reported previously.<sup>22–24</sup> When pressure exceeds 54 Mbar, we find that the 12-atom per unit cell *Cmcm* structure of Ref. 22, hereafter *Cmcm*-12, becomes less stable than a new *Cmcm*-4 structure, in which three groups of bonds (different in length) exist without forming in-plane H<sub>3</sub> clusters.<sup>22</sup> As pressure increases to 87 Mbar, the hexagonal close packed (hcp) structure (symmetry *P6<sub>3</sub>/mmc*) becomes stable. Different from the *P6<sub>3</sub>/mmc* structure predicted in Ref. 23 ( $c/a \approx 2$ ), our hcp lattice exhibits a smaller  $c/a$  ratio of 1.58. The hcp structure remains stable until being replaced by the face-centered cubic (fcc) lattice at 180 Mbar.

Having computed the ground-state structures of H and H<sub>2</sub>O throughout a wide pressure range, we now explore novel hydrogen-oxygen stoichiometries, including hydrogen-enriched structures H<sub>3</sub>O, H<sub>4</sub>O, H<sub>6</sub>O, and H<sub>8</sub>O and oxygen-rich structures HO, HO<sub>2</sub>, and HO<sub>4</sub>. Between 200 and 3000 random structures with up to 8 f.u. at pressures of 20–500 Mbar were generated, depending on the specific computational cost and searching efficiency. We have only considered crystalline compounds in this study. Any defects, stacking faults, or other nonstoichiometric arrangements of atoms have been neglected because this study is focused on the ground state.

Figure 3 compares the stability of structures with different stoichiometries using a convex hull diagram.<sup>25</sup> This diagram shows the enthalpy of formation (EOF) per atom,  $E_f$ , of the most stable H<sub>*m*</sub>O<sub>*n*</sub> compounds with respect to the elements. For each fractional concentration of oxygen,  $x = n/(m + n)$ , a compound H<sub>*m*</sub>O<sub>*n*</sub> is stable relative to separate A and B phases (A + B) of different concentrations if its EOF lies

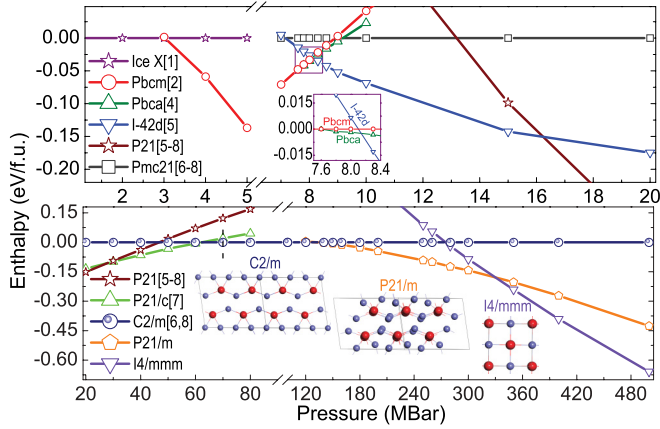


FIG. 1. (Color online) Enthalpy versus pressure of different water ice structures. The reference following the name of each phase is the corresponding earliest report. In the lower panel, structures are provided for  $C2/m$ ,  $P2_1/m$ , and  $I4/mmm$ , where large red and small blue spheres represent O and H atoms, respectively. The dashed line at 70 MBar indicates the highest pressure explored in previous work.

below the line connecting those two phases. This approach is valid for determining structural stability at zero temperature, when the Gibbs free energy is equivalent to the enthalpy. In Fig. 3(a) we plot a convex hull diagram showing the EOF of possible H-O phases at a pressure of 100 Mbar. The H<sub>4</sub>O structure emerges as the most stable on the hydrogen-enriched side of the diagram, implying that any H-O complex with an H:O concentration greater than 2:1 will preferentially form H<sub>4</sub>O + H or H<sub>4</sub>O + H<sub>2</sub>O, in contrast to H<sub>2</sub>O + H<sub>2</sub> we expect at ambient pressure. On the oxygen-rich side of the graph, the HO, HO<sub>2</sub>, and HO<sub>4</sub> phases are unstable relative to H<sub>2</sub>O + O.

In Fig. 3(b) we focus on the EOF of hydrogen-enriched compounds including the H<sub>3</sub>O and H<sub>4</sub>O phases, with respect to their end members H and H<sub>2</sub>O. Based on our calculations at 10 and 20 Mbar, we predict H<sub>4</sub>O to become stable relative

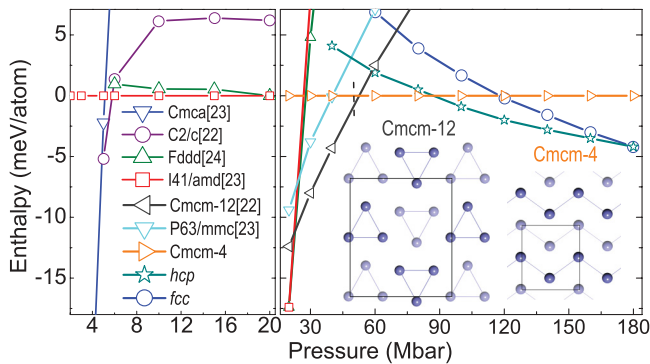


FIG. 2. (Color online) Enthalpy versus pressure of different structures of hydrogen relative to  $I4_1/amd$ <sup>23</sup> in the left panel and the 4-atom  $Cmcm$  phase on the right. Zero-point energy (ZPE) is not included. The reference for each phase is given in the legend. In the right panel, structures of the 12-atom  $Cmcm$  of Ref. 22 and our new 4-atom  $Cmcm$  are compared. The dashed line at 50 MBar indicates the highest pressure explored in previous work. Note that ZPE differences between hydrogen structures can be sufficient to change their relative ordering.

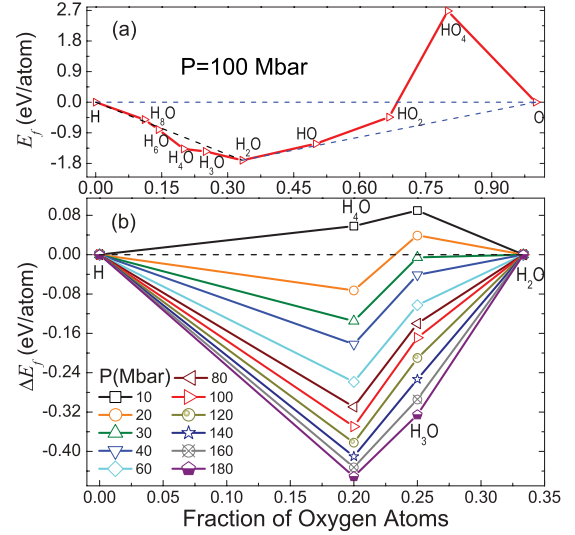


FIG. 3. (Color online) (a) Enthalpy of formation (EOF) of different H-O compounds with respect to H and O at 100 Mbar. (b) EOF of hydrogen-rich H-O compounds with respect to H and H<sub>2</sub>O at several pressures.

to H + H<sub>2</sub>O at 14 Mbar. Such a pressure is predicted to be for the core-mantle boundary (CMB) of Saturn and far below that of Jupiter. For pressures above 140 Mbar, we find H<sub>3</sub>O becoming stable relative to H<sub>2</sub>O + H<sub>4</sub>O. These results imply that at giant-planet CMB pressures, in the absence of temperature effects, hydrogen and oxygen exist in the form of the novel hydrogen-rich compound, H<sub>4</sub>O, instead of separate water ice and hydrogen. On the other hand, no oxygen-rich compounds will form, which is in agreement with recent calculations at high temperatures.<sup>26</sup>

The H<sub>4</sub>O phase that we find here is a layered orthorhombic structure with  $Pnma$  symmetry. Each layer is characterized by -H-O-H-O- chains, of which each O is associated with one H<sub>3</sub> unit shown in Fig. 4. For H<sub>3</sub>O, we find a body-centered cubic (bcc) structure ( $Im\bar{3}m$ ) above 110 Mbar, a layered monoclinic  $C2/m$  structure (see Fig. 5) at 20–110 Mbar, and a slightly less stable orthorhombic  $Cmmm$  structure (see Fig. 6) between 20 and 100 Mbar, whose enthalpy is very close (2–36 meV/f.u.) to that of the  $C2/m$  structure. Our band structure analysis showed that the H<sub>4</sub>O structure becomes metallic at 80 Mbar. This metallization pressure is higher than what has been reported for hydrogen (4–5 Mbar<sup>27</sup>) and H<sub>2</sub>O (about 60 Mbar).

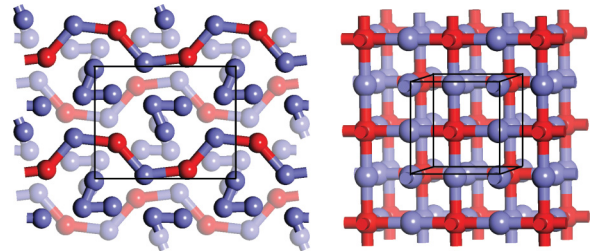


FIG. 4. (Color online) Structures of H<sub>4</sub>O- $Pnma$  (left) and H<sub>3</sub>O-bcc (right). Red and blue spheres denote oxygen and hydrogen atoms, respectively.

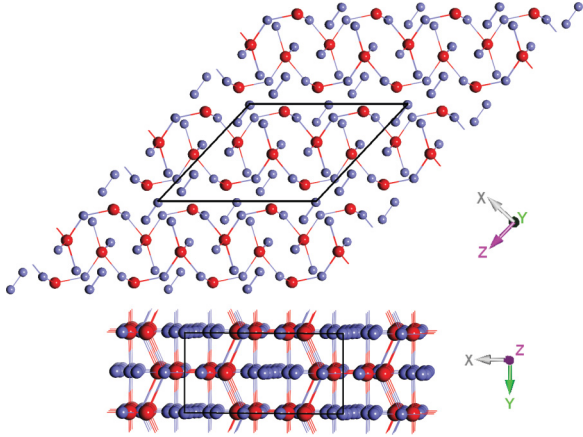


FIG. 5. (Color online)  $\text{H}_3\text{O}-C2/m$  structure, characterized by atomic layers connected by H-O chains that are either straight or zigzag. Red and blue spheres denote oxygen and hydrogen atoms, respectively.

To verify the applicability of the PAW pseudopotential under extreme pressures, we performed all-electron LAPW calculations using the ELK code.<sup>28</sup> The LAPW calculations for hydrogen at 80–180 Mbar reconfirm the  $Cmcm \rightarrow hcp$  transition at 87 Mbar and increase the enthalpy of the fcc structure by 5 meV, precluding fcc to become stable until a pressure of about 200 Mbar is reached. We also recalculated the EOF of  $\text{H}_3\text{O}$  with respect to H and  $\text{H}_2\text{O}$  at 100 Mbar, and found that the difference between the two methods is only 4 meV/f.u. We further replaced the VASP-PAW pseudopotential of oxygen with an all-electron PAW potential (cutoff radius equals to 0.95 Bohr), reoptimized two  $\text{H}_2\text{O}$  structures,  $I4/mmm$  and  $C2/m$ , and compared their enthalpy. The enthalpy difference between the  $I4/mmm$  and the  $C2/m$  structures increases by 16 and 70 meV/f.u. at 180 and 400 Mbar, respectively. All these corrections are small and confirm our prediction of two new ice phases, although their transition pressures increase slightly (by <4% for  $P2_1/m$ , <18% for  $I4/mmm$ ).

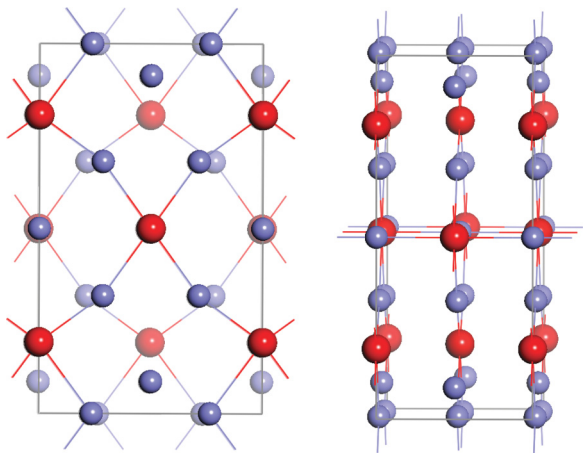


FIG. 6. (Color online)  $\text{H}_3\text{O}-Cmmm$  structure, consisting of H-O atomic planes that are connected by straight H-O chains. Red and blue spheres denote oxygen and hydrogen atoms, respectively. Different color depth in the left panel corresponds to different atomic planes.

TABLE II. Zero-point energy (ZPE) of H (in units of eV/atom), and of  $\text{H}_2\text{O}$ ,  $\text{H}_3\text{O}$ , and  $\text{H}_4\text{O}$  (in units of eV/f.u.) structures at 20 and 180 Mbar.

Structure	ZPE (20 Mbar)	ZPE (180 Mbar)
H- $I4_1/amd$	0.443	
$\text{H}_2\text{O}-P2_1$	1.268	
$\text{H}_3\text{O}-Cmmm$	1.725	
$\text{H}_4\text{O}-Pnma$	2.213	4.603
H-fcc ( $Fm\bar{3}m$ )		0.830
$\text{H}_2\text{O}-P2_1/m$		2.571
$\text{H}_3\text{O}-bcc (Im\bar{3}m)$		3.756

We also estimated the influence of zero-point motion (ZPM) by phonon calculations with  $2 \times 2 \times 2$  supercells using the finite displacement method.<sup>29</sup> Including zero-point energy (ZPE, see Table II), the convex hull diagram in Fig. 3(b) shifts in the positive direction by 12 meV/atom for  $\text{H}_4\text{O}$  and 3 meV/atom for  $\text{H}_3\text{O}$  at 20 Mbar, and by 74 meV/atom for  $\text{H}_4\text{O}$  and 89 meV/atom for  $\text{H}_3\text{O}$  at 180 Mbar. By applying these changes to the linearly interpolated enthalpy, we estimate the ZPM increases the pressure at which  $\text{H}_4\text{O}$  and  $\text{H}_3\text{O}$  become more stable than their corresponding H +  $\text{H}_2\text{O}$  by, at most, 1.3 Mbar. Relative to  $\text{H}_2\text{O}$  +  $\text{H}_4\text{O}$ ,  $\text{H}_3\text{O}$  becomes less stable below 180 Mbar. We note that, based on the findings in Refs. 6,8, the ZPM-induced changes in the enthalpy differences between  $\text{H}_2\text{O}$  structures are small and do not change the sequence of phase transition, although the transition pressures will be slightly affected. Further, although the ZPE difference between different hydrogen structures can be sufficient to change the relative ordering, the difference is small (<80 meV/atom when below 50 Mbar), as indicated in Ref. 23, and will not change our conclusions on the stability of  $\text{H}_4\text{O}$ .

In this work we have replicated and extended the phase diagram of solid hydrogen to 180 Mbar and that of water ice to 500 Mbar. We also predict novel, hydrogen-enriched meta-ice structures to become more stable than separate hydrogen and water ice phases at high pressure. Our results imply that under conditions in excess of 14 Mbar at low temperature a hydrogen-rich  $\text{H}_4\text{O}$  phase exists instead of separate water ice and hydrogen phases. The 14 Mbar pressure in question is comparable to the CMB of Saturn and far below the core pressure of Jupiter, and may potentially also be reached inside super-Neptune ice giants. This result stands in contrast to the tendency of methane to preferentially expel hydrogen from its own structure under pressure to form hydrocarbons and eventually diamond,<sup>30</sup> and in ice mixtures methane could potentially provide the excess hydrogen to form  $\text{H}_4\text{O}$ . These results underline the fact that chemistry at high pressure may deliver substantially counterintuitive results, and that consideration of structures likely to form at giant-planet core conditions requires looking beyond traditional ambient-pressure chemistry to explore unfamiliar stoichiometries and combinations of elements.

This work was supported by NASA and the NSF. The computation was performed using LBNL and UC-Berkeley resources. S.Z. acknowledges support from a graduate student fellowship of the EPS department.



\*shuai.zhang01@berkeley.edu

†militzer@berkeley.edu

- <sup>1</sup>A. Polian and M. Grimsditch, *Phys. Rev. Lett.* **52**, 1312 (1984).
- <sup>2</sup>M. Benoit, M. Bernasconi, P. Focher, and M. Parrinello, *Phys. Rev. Lett.* **76**, 2934 (1996).
- <sup>3</sup>W. B. Hubbard, *Planetary Interiors* (University of Arizona Press, Tucson, 1984).
- <sup>4</sup>B. Militzer and H. F. Wilson, *Phys. Rev. Lett.* **105**, 195701 (2010).
- <sup>5</sup>Y. Wang, H. Liu, J. Lv, L. Zhu, H. Wang, and Y. Ma, *Nature Commun.* **2**, 563 (2011).
- <sup>6</sup>J. M. McMahon, *Phys. Rev. B* **84**, 220104 (2011).
- <sup>7</sup>M. Ji, K. Umemoto, C.-Z. Wang, K.-M. Ho, and R. M. Wentzcovitch, *Phys. Rev. B* **84**, 220105 (2011).
- <sup>8</sup>A. Hermann, N. W. Ashcroft, and R. Hoffmann, *Proc. Natl. Acad. Sci. U.S.A.* **109**, 745 (2012).
- <sup>9</sup>K. Umemoto and R. M. Wentzcovitch, *Earth Planet. Sci. Lett.* **311**, 225 (2011).
- <sup>10</sup>C. J. Pickard and R. J. Needs, *J. Phys.: Condens. Matter* **23**, 053201 (2011).
- <sup>11</sup>C. J. Pickard and R. J. Needs, *Phys. Rev. Lett.* **97**, 045504 (2006). *Nature Mater.* **7**, 775 (2008).
- <sup>12</sup>A. J. Morris, C. J. Pickard, and R. J. Needs, *Phys. Rev. B* **80**, 144112 (2009).
- <sup>13</sup>A. D. Fortes, E. Suard, M.-H. Lemée-Cailleau, C. J. Pickard, and R. J. Needs, *J. Am. Chem. Soc.* **131**, 13508 (2009).
- <sup>14</sup>G. Kresse and J. Furthmüller, *Comput. Mater. Sci.* **6**, 15 (1996). *Phys. Rev. B* **54**, 11169 (1996).
- <sup>15</sup>G. Kresse and D. Joubert, *Phys. Rev. B* **59**, 1758 (1999).
- <sup>16</sup>J. P. Perdew, K. Burke, and M. Ernzerhof, *Phys. Rev. Lett.* **77**, 3865 (1996).
- <sup>17</sup>H. J. Monkhorst and J. D. Pack, *Phys. Rev. B* **13**, 5188 (1976).
- <sup>18</sup>J. D. Pack and H. J. Monkhorst, *Phys. Rev. B* **16**, 1748 (1977).
- <sup>19</sup>M. Martinez-Canales, C. J. Pickard, and R. J. Needs, *Phys. Rev. Lett.* **108**, 045704 (2012).
- <sup>20</sup>J. Sun, M. Martinez-Canales, D. D. Klug, C. J. Pickard, and R. J. Needs, *Phys. Rev. Lett.* **108**, 045503 (2012).
- <sup>21</sup><http://cst-www.nrl.navy.mil/lattice/struk/lp2.html>.
- <sup>22</sup>H. Liu, H. Wang, and Y. Ma, *J. Phys. Chem. C* **116**, 9221 (2012).
- <sup>23</sup>J. M. McMahon and D. M. Ceperley, *Phys. Rev. Lett.* **106**, 165302 (2011).
- <sup>24</sup>H. Y. Geng, H. X. Song, J. F. Li, and Q. Wu, *J. Appl. Phys.* **111**, 063510 (2012).
- <sup>25</sup>I. Opahle, G. K. H. Madsen, and R. Drautz, *Phys. Chem. Chem. Phys.* **14**, 16197 (2012).
- <sup>26</sup>H. F. Wilson and B. Militzer, *Astrophys. J.* **745**, 54 (2012).
- <sup>27</sup>H.-K. Mao and R. J. Hemley, *Rev. Mod. Phys.* **66**, 671 (1994).
- <sup>28</sup><http://elk.sourceforge.net/>.
- <sup>29</sup>D. Alfè, *Comput. Phys. Commun.* **180**, 2622 (2009).
- <sup>30</sup>F. Ancilotto, G. L. Chiarotti, S. Scandolo, and E. Tosatti, *Science* **275**, 1288 (1997).